

# Optimization and performance of cost-effective ultra-high performance concrete

Weina Meng · Mahdi Valipour ·  
Kamal Henri Khayat

Received: 19 February 2016 / Accepted: 26 May 2016 / Published online: 10 August 2016  
© RILEM 2016

**Abstract** This paper presents a mix design method for ultra-high performance concrete (UHPC) prepared with high-volume supplementary cementitious materials and conventional concrete sand. The method involves the optimization of binder combinations to enhance packing density, compressive strength, and rheological properties. The water-to-cementitious materials ratio is then determined for pastes prepared with the selected binders. The sand gradation is optimized using the modified Andreasen and Andersen packing model to achieve maximum packing density. The binder-to-sand volume ratio is then determined based on the void content, required lubrication paste volume, and compressive strength. The optimum fiber volume is selected based on flowability and flexural performance. The high-range water reducer dosage and  $w/cm$  are then adjusted according to the targeted mini-slump flow and compressive strength. Finally, the optimized UHPC mix designs are evaluated to determine key properties that are relevant to the intended application. This mix design approach was applied to develop cost-effective UHPC materials. The results indicate that the optimized UHPC can develop 28-days compressive

strength of 125 MPa under standard curing condition and 168–178 MPa by heat curing for 1 days. Such mixtures have unit cost per compressive strength at 28 days of 4.1–4.5 \$/m<sup>3</sup>/MPa under standard curing.

**Keywords** Conventional concrete sand · Cost-effective · Mix design · Rheological properties · Supplementary cementitious materials (SCMs) · Ultra-high performance concrete (UHPC)

## 1 Introduction

With appropriate combination of cementitious materials, adequate sand gradation, and incorporation of fiber reinforcement and high-range water reducer (HRWR), ultra-high performance concrete (UHPC) can be produced to deliver high flowability (self-consolidating), mechanical properties, and durability [1, 2]. However, high material cost is restricting UHPC's wider acceptance worldwide [3–5]. Development of cost-effective UHPC is crucial for greater acceptance of this novel construction material.

High-volume replacement of cement with sustainable supplementary cementitious materials (SCMs), such as fly ash, ground granulated blast furnace slag (GGBS), and silica fume (SF), can be performed to reduce cement content without significantly sacrificing the mechanical strengths [5–8]. Mixtures containing 20–35 % (vol.%) GGBS, 10–30 % Class C fly ash (FAC), and 15–30 % SF have been used in

---

W. Meng · M. Valipour · K. H. Khayat (✉)  
Department of Civil, Architectural, and Environmental  
Engineering, Missouri, University of Science and  
Technology, 205 ERL 500 W 16th street, Rolla,  
MO 65409, USA  
e-mail: khayatk@mst.edu

proportioning UHPC [5–8]. However, the substitution ratios were relatively low. A high-volume substitution of SCMs in proportioning UHPC need to be further investigated to reduce material costs.

Ground quartz sands (0–0.6 mm) are typically used for producing UHPC [9, 10]. Conventional concrete sand was used to replace quartz sand and reduce the initial unit cost. Yang et al. [11] used two types of locally natural sand to replace finely ground quartz sand. Experimental results indicated that the use of natural sand led to reduction in compressive strength and fracture energy of about 15 % lower than those of UHPC made with quartz sand. Wang et al. [8] reported that the 91-days compressive strength could achieve 150 MPa or higher strength when conventional concrete sand was used. However, high-volume SF (25 %, by volume) was used. Besides, reducing the binder content can decrease unit cost of UHPC. The binder content can be reduced by optimizing the sand gradation to achieve a higher packing density [12]. Appropriate binder contents need to be investigated in order to strike a balance between mechanical properties and unit cost of UHPC.

Reducing the steel fiber content is also vital in reducing unit cost of UHPC [9]. While steel fibers greatly enhance tensile properties of UHPC, they import an adverse effect on flowability. An optimum content of steel fibers should be adopted to balance the workability, and mechanical performance [9, 13]. An effective mix design method is of great importance for UHPC proportioning. The mix design should involve combining optimum proportions of all mixture constituents to fulfill the requirements of fresh and hardened concrete for a particular application [14]. In general, two methodologies exist for UHPC mix design. The first approach seeks to reduce porosity by decreasing the water-to-cementitious ratio, by mass, (w/cm) [2, 15], and applying high temperature/pressure curing or vacuum mixing [16]. However, the reduction in w/cm may lead to a high amount of entrapped air, negatively affecting mechanical properties [9]. High temperature/pressure curing or vacuum mixing may not be practical for cast-in-place applications. The second approach for UHPC mix design involves the increase in packing density [1, 5]. A modified Andreasen and Andersen model was employed to optimize UHPC mix design [17]. The binder combinations and sand gradations were adjusted to achieve the best fit to the target particle

size distribution proposed by the modified Andreasen and Andersen model using a least square method [5, 18]. However, the significant effects of water and chemical admixture on packing density of fine particles (<100  $\mu\text{m}$ ) were not considered and only the solid materials were taken into account. The packing density of cementitious materials is strongly dependent on the water addition and dispersion imported by the use of HRWR [19]. Since the interparticle cohesive forces, especially electrostatic and Van der Waals forces, far exceed the gravitational forces, flocculation can form and compromise the packing [20]. A slight increase in free moisture content around fine particles can enhance packing. Water on particle surfaces can lead to lubrication and act as electrical conductor to relieve interparticle forces [21]. Considering the presence of water, the packing density should be determined under wet conditions [19]. However, packing models are still applicable for sand since sand particles are relatively large, and the gravitational forces far exceed the cohesive forces. Therefore, the packing densities of cementitious materials and sand should be analyzed separately.

A systematic mix design procedure was developed and implemented, incorporating preliminary testing and mathematical models. The mix design aims at achieving a densely-compacted cementitious matrix for UHPC with enhanced fresh and mechanical properties and relatively low cost. A number of cost-effective UHPC mixtures, which have high-volume SCMs, conventional concrete sand, and relatively low fiber content, are proposed and evaluated in terms of key workability, shrinkage, and durability characteristics.

## 2 Materials, mixers, and specimen preparations

In this study, the cementitious materials included FAC, GGBS, SF, and Type III Portland cement. The characteristics of the investigated raw materials are listed in Table 1. Fine SF with particles smaller than 1  $\mu\text{m}$  in diameter was used; the mean diameter of the SF is about 0.15  $\mu\text{m}$ , and the specific surface area determined using the Brunauer, Emmet, and Teller (BET) method is 18,500  $\text{m}^2/\text{kg}$ . Missouri River sand (0–4.75 mm) and masonry sand (0–2.00 mm) were used under saturated surface dry (SSD) condition. The water absorptions of the river sand and masonry sands are 0.14 and 0.06 %, respectively. A polycarboxylate



**Table 1** Characteristics of raw materials

	Type III Portland cement	Class C fly ash	Silica fume	GGBS	Missouri river sand	Masonry sand
SiO <sub>2</sub> (%)	19.72	36.5	95.5	36.8	80.3	86.5
Al <sub>2</sub> O <sub>3</sub> (%)	5.10	24.8	0.7	9.2	10.5	0.39
Fe <sub>2</sub> O <sub>3</sub> (%)	2.76	5.2	0.3	0.76	3.43	1.47
CaO (%)	64.50	28.1	0.4	37.1	1.72	9.42
MgO (%)	2.30	5	0.5	9.5	1.70	0
SO <sub>3</sub> (%)	3.25	2.5	0	0.06	1.07	0
Na <sub>2</sub> O eq. (%)	0.33	0	0.4	0.34	–	0
C <sub>3</sub> S (%)	65.23	–	–	–	–	–
C <sub>2</sub> S (%)	7.33	–	–	–	–	–
C <sub>3</sub> A (%)	8.85	–	–	–	–	–
C <sub>4</sub> AF (%)	8.40	–	–	–	–	–
Loss of ignition (%)	2.6	0.3	2.6	5.1	1.28	0.24
Blaine surface area (m <sup>2</sup> /kg)	562	465	–	589	–	–
B.E.T. (m <sup>2</sup> /kg)	–	–	18,200	–	–	–
Specific gravity	3.15	2.70	2.20	2.90	2.65	2.64

HRWR was used to enhance the workability. The HRWR has a solid mass content of 23 % and a specific gravity of 1.05. Straight steel fibers with 0.2-mm diameter and 13-mm length were used to enhance mechanical properties. The tensile strength and elastic modulus of the steel fiber are 1.9 and 203 GPa, respectively.

All mixtures were prepared and tested at room temperature ( $23 \pm 2$  °C). Two mixers were used which were a 12-L Hobart mixer and a 150-L EIRICH mixer. The Hobart mixer was used for optimizing the individual components for UHPC, and the EIRICH mixer was employed for finalizing the UHPC mixtures. A specific mixing procedure was employed for each mixer. When the Hobart mixer was used, the mixing procedure was composed of three steps: (1) dry cementitious materials or/and sand were mixed for 2 min at 1 rps; (2) 90 % of the mixing water and 90 % of the HRWR were added and the mixture was mixed for 3 min at 2 rps; (3) the rest of water and HRWR were added and the mixture was mixed for 9 min at 2 rps. When the EIRICH mixer was used, the mixing procedure was composed of five steps: (1) the mixer was pre-wetted; (2) the sand and cementitious materials were added into the mixer and mixed for 2 min at 1 rps; (3) 90 % of the total liquid (water + HRWR), by volume, was added and mixed for 2 min at 6 rps; (4) the rest of the liquid was introduced, and the

materials were mixed for 4 min at 6 rps; (5) the fibers were added gradually over a period of 1 min; (6) the materials were mixed for 2 min at 10 rps. While mixing, the pan speed of the mixer was fixed at 2 rps.

For each mixture, specimens were cast in one lift without mechanical consolidation. The molds were immediately covered after casting with wet burlaps and plastic sheets. They were demolded after 1 days, and then cured in lime-saturated water at  $23 \pm 1$  °C until the time of testing (standard curing). To investigate the effects of curing on compressive strength, two sets of UHPC specimens were prepared and tested, one set with standard curing and the other set with heat curing. Heat curing was performed at a maximum temperature of 90 °C for 24 h. The specimens were then cured in lime-saturated water for 7 days, followed by air-curing at room temperature.

### 3 Proposed mix design procedure and experimental program

The proposed UHPC mix design method consists of six main steps, as illustrated in Fig. 1: (1) determine binder candidates; (2) preliminarily select a w/cm; (3) determine the sand combination; (4) assess the binder-to-sand volume ratio ( $V_b/V_s$ ); (5) optimize the fiber content; and (6) evaluate and adjust the UHPC



mixture. Step 1 is composed of three sub-steps: (1a) select binder combination candidates based on flow characteristics; (1b) narrow down the binder candidates according to the combined effects of minimum water content (MWC), relative water demand (RWD), and HRWR demand, as well as 1- and 28-days compressive strengths; (1c) finalize the binder combinations based on the rheological properties.

### 3.1 Step 1: Optimize binder combinations for paste

With the initially-selected binder combinations, which aim at using high-volume SCMs in proportioning UHPC, flow tests are conducted to evaluate the MWC and RWD of binders under wet conditions in order to screen candidates for binders. The paste mixtures with lower MWC are advantageous in terms of the packing density, and thus, the corresponding binders are selected for further optimization. To further narrow down the candidates of the optimum binder combinations, the HRWR demand and compressive strength of the binders selected based on flow characteristics are then evaluated. For a given sand and fiber content, any

change in the rheological characteristics are directly related to the changes of the paste matrix [22]. Therefore, final binder selection is based rheological properties of the successful binder systems. The three sub-steps are elaborated as follows.

#### 3.1.1 Sub-step 1a: Select binder candidates based on flow characteristics for paste

A mini-slump test is conducted in accordance with ASTM C 230/C 230 M. For each of the test binders, seven mixtures are prepared with various water-to-binder ratio (w/b), by volume, values ranging from 0.4 to 1.0. This is carried out to establish a relationship between fluidity and w/b for each binder combination, as illustrated in Fig. 2. The intercept on the vertical axis represents the MWC required to initiate flow, and the slope of the relationship represents the RWD. Assuming there is no air entrapped in the paste, the volume occupied by the water content can be taken as the minimum void content. Therefore, a low MWC represents a high packing density of the binder [23]. A high RWD indicates that a given increase in w/b can result in small impact on the flowability. Thus, mixtures with

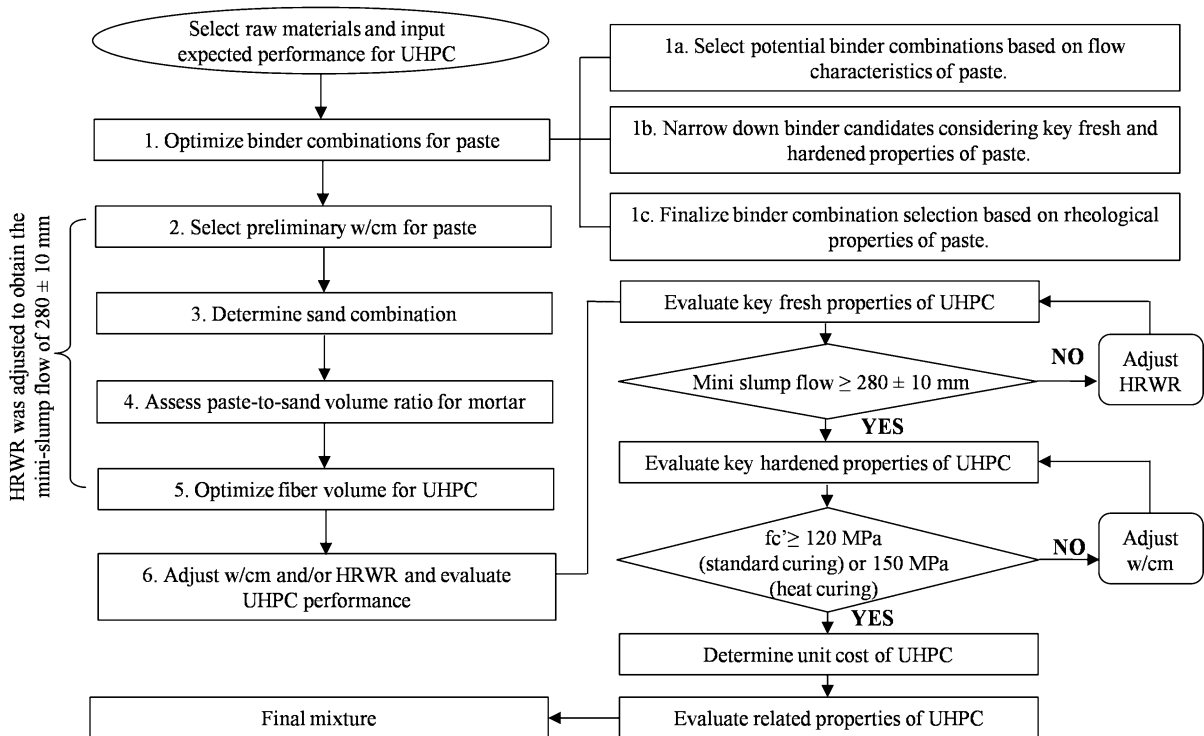


Fig. 1 Procedure of mix design methodology for UHPC



high RWD are more robust to variations in water content [23]. Therefore, binder combinations with low MWC and high RWD are desirable for designing UHPC.

### 3.1.2 Sub-step 1b: Narrow down binder candidates based on key fresh and hardened properties for paste

To further narrow down the binder combinations, key fresh and hardened properties of the selected binder combinations are evaluated. The 1- and 28-days compressive strengths are measured in accordance with ASTM C 109. The HRWR dosage is adjusted to obtain a mini-slump flow of  $280 \pm 10$  mm, which is commonly adopted to ensure good flowability and low air entrapment [24]. The flow time is measured using a mini-V funnel in accordance with the [25]. The mixtures with higher compressive strength and lower HRWR demand are preferred.

A radar chart is employed to display multivariate criteria for the selection of binder [26]. The criteria include the MWC, RWD, HRWR demand, and 1- and 28-days compressive strengths. The plot consists of a sequence of equi-angular spokes (radii), and each spoke represents one variable (see Fig. 5, Sect. 4.1). The length of each spoke is proportional to the magnitude of the corresponding variable. Each variable is assigned with a specific weight factor. The data points of each spoke are sequentially connected and formed a specific area. A larger area indicates a better performance of the mixture [26].

### 3.1.3 Sub-step 1c: Finalize the binder selection based on the rheological properties for paste

The rheological properties of paste mixtures with the selected binders in Sub-step 1b are tested using a co-

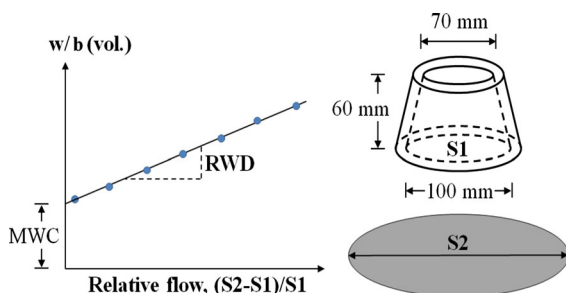


Fig. 2 MWC and RWD in the mini-slump flow test

axial rheometer (Anton Paar MCR 302) at different ages, up to 60 min. The w/b is fixed at 0.63, which corresponds to a w/cm of 0.20, for mixture made with 100 % Portland cement. The mini-slump spread value is fixed at  $280 \pm 10$  mm by adjusting the HRWR dosage.

The plastic viscosity ( $\mu_p$ ) is measured at 20, 40 and 60 min after water addition. The paste in the rheometer undergoes a 60-s pre-shearing period at a shear rate of  $100 \text{ s}^{-1}$ . This operation could minimize the structural build-up of paste at rest. Then, the shear rate is reduced by  $10 \text{ s}^{-1}$  for every 5 s until zero. The dynamic yield stress ( $\tau_0$ ) and  $\mu_p$  are calculated using the Bingham fluid model [27], as shown in Eq. 1:

$$\tau = \tau_0 + \mu_p \dot{\gamma} \quad (1)$$

where  $\dot{\gamma}$  denotes the shear rate. A relatively low value of  $\mu_p$  is more desirable to ensure the proper filling capacity.

### 3.2 Step 2: Preliminarily select a w/cm for paste

The w/cm of UHPC is typically in the range of 0.15–0.25 [9]. Paste mixtures of the selected binder combinations were proportioned with w/cm ranging between 0.18 and 0.23. The selection of the appropriate w/cm is based on HRWR demand and 28-days compressive strength under standard curing. The selected w/cm is applied in the later investigations to determine the optimum sand and fiber content (see Steps 3 and 4). The preliminary w/cm may be slightly adjusted in the final UHPC mixtures to achieve good balance between flowability and strength which is elaborated in Step 6.

### 3.3 Step 3: Determine sand gradation

The modified Andreasen and Andersen model acts as a targeted function for the optimization of sand gradation, as shown in Eq. 2 [17]:

$$P(D) = \frac{D^q - D_{\min}^q}{D_{\max}^q - D_{\min}^q} \quad (2)$$

where  $P(D)$  represents the weight percentage of sand passing the sieve with size  $D$ ,  $D_{\max}$  is the maximum particle size ( $\mu\text{m}$ ),  $D_{\min}$  is the minimum particle size ( $\mu\text{m}$ ), and  $q$  is the distribution modulus which is related to the sand particle size. For fine particles,  $q$  can be set

at 0.23 ( $q < 0.25$ ) [5]. The sand proportions are adjusted until the best fit is achieved between the composed gradation and the targeted curve, using an optimization algorithm based on the least square method. When the discrepancy between the targeted curve and the composed sand gradation is minimized, the sand combination can be considered as optimum.

According to the excess thickness theory [28], the fluid paste volume should be high enough to fill voids between sand particles and provide a lubrication layer that envelops the particles to achieve a high flowability [29]. The bulk density of the compacted sand blend can be determined using a Gyrator compactor testing machine. A sand sample can be compacted by a continuous kneading action consisting of axial pressure and shear. The applied overhead air pressure is set at  $4 \pm 10^5$  Pa. The gyrator angle and cycle number are fixed at  $2^\circ$  and 200, respectively. The working speed is 1 rps. The void content ( $\alpha$ ) of the compacted sand blend can be then be calculated as:

$$\alpha = (1 - \gamma_{RM}/\rho_{RM}) \times 100 \quad (3)$$

$$\rho_{RM} = \rho_{Ri} \times \sum_{i=1}^n (V_{Ri}/V_{RM}) \quad (4)$$

where  $\gamma_{RM}$  is the bulk density of dry sand blend,  $V_{Ri}$  and  $V_{RM}$  are absolute volumes of river sand and sand blend, respectively, and  $\rho_{Ri}$  and  $\rho_{RM}$  are the densities of river sand and sand blend, respectively.

### 3.4 Step 4: Determine $V_b/V_S$ of mortar

The primary paste volume, denoted by  $V_b$ , takes into account the paste volume that is necessary to fill the void content of the sand and lubricate the sand particles. The primary paste can be calculated using the approach proposed by Koehler and Fowler [29]:

$$V_b = V_{exp} + V_{void} \quad (5)$$

$$V_{exp} = 8 + (16 - 8)/2(R_{S,A} - 1) \quad (6)$$

$$V_{void} = \alpha(100 - V_{exp})/100 \quad (7)$$

$$V_S = (V_{exp} + V_{void})/(100 - V_{exp} - V_{void}) \quad (8)$$

where  $V_S$  expresses as the sand volume,  $V_{exp}$  denotes excess paste volume (vol.%),  $V_{void}$  is void content in mortar (vol.%), and  $R_{S,A}$  is a coefficient related to the shape and the angularity of sand in the range of 1–5 [29].

The minimum  $V_b/V_S$  value can provide the necessary paste for filling ability. However, the minimum value is not necessarily appropriate for a specific requirement of strength. Therefore, additional experiments need to be carried out to validate the optimum value of  $V_b/V_S$  using mortar mixtures. The 28-days compressive strength of each mortar mixture with a  $V_b/V_S$  value can be evaluated. The HRWR dosage is adjusted to obtain a mini-slump flow of  $280 \pm 10$  mm.

### 3.5 Step 5: Determine fiber content of UHPC

The fiber content of UHPC commonly ranges from 2 to 5 % [30]. The optimum fiber content is determined based on key fresh and mechanical properties of UHPC mixtures made with different fiber contents. The mini-V-funnel and mini-slump tests are used to express workability. The HRWR dosage is adjusted to obtain a mini-slump flow of  $280 \pm 10$  mm. Flexural load–deflection relationships are determined in accordance with ASTM C 1609 to evaluate the first cracking strength and load capacity. Beam specimens ( $304.8 \times 76.2 \times 76.2$  mm<sup>3</sup>) are tested after 28-days standard curing.

### 3.6 Step 6: Adjust w/cm and/or HRWR and evaluate performance of UHPC

In this step, trial batches are prepared to verify compliance of selected mixtures with mini-slump flow of  $280 \pm 10$  mm and 28-days compressive strength  $\geq 120$  MPa under standard curing and/or  $\geq 150$  MPa under heat curing. If the mixture does not achieve the targeted performance, either the HRWR dosage or w/cm can be adjusted. For the selected mixture(s), key properties of the UHPC should be determined, as elaborated below.

#### 3.6.1 Fresh properties

The HRWR dosage is adjusted to secure an initial mini-slump flow of  $280 \pm 10$  mm. The unit weight and air content are measured in accordance with ASTM C 138 and ASTM C 231, respectively. The initial and final setting times are tested in accordance with ASTM A403.

A ConTech 5 viscometer can be employed to determine  $\tau_0$  and  $\mu_p$  of the UHPC. Typically, the



measurements begin at 10 min after water addition with samples subjected to pre-shear at a rotational velocity of 0.50 rps during 25 s, followed by a stepwise reduction in rotational velocity. The  $\tau_0$  and  $\mu_p$  are then calculated using the Bingham fluid model [27], as shown in Eq. 1.

### 3.6.2 Mechanical properties

Compressive strength and flexural properties can be tested at different ages. The elastic modulus can be determined in accordance with ASTM C 469. The splitting tensile strength can be measured in accordance with ASTM C 496. Three samples are replicated in each test.

### 3.6.3 Autogenous and drying shrinkage

The autogenous shrinkage can be evaluated in accordance with ASTM C 1698 using samples in corrugated plastic tubes and stored immediately after casting at  $20 \pm 0.5$  °C and  $50 \pm 2$  % RH. The first measurement is taken as final setting. The second measurement is taken at 12 h after final setting. Other measurements are carried out daily within the 1st week, and then, weekly until 28 days after final setting. Drying shrinkage can be evaluated using prism specimens in accordance with ASTM 596, until 91 days after 7-days moist curing.

### 3.6.4 Durability

If deemed necessary, some durability characteristics of the optimized UHPC mixture can be investigated. For example, electrical resistivity can be measured in accordance with ASTM C 1760, and frost durability can be determined in accordance with the ASTM C 666, Procedure A.

## 4 Experimental validations

As stated earlier, the study aimed at using high-volume SCMs and locally available conventional concrete sand in proportioning UHPC to reduce the material's unit cost. An example of using the mix design method in detail is presented as follows.

### 4.1 Optimize binder combinations for paste

#### 4.1.1 Select binder candidates based on flow characteristics of paste

The initial binder combinations contained SF  $\leq 25$  %, vol.%, and FAC or/and GGBS  $\geq 30$  %, vol.%, as listed in Table 2. In total, 27 binder systems were investigated, which consisted of the reference, 14 binary, nine ternary, and three quaternary binders. The binary binders were categorized into three groups: (i) four GGBS systems, (ii) four FAC systems, and (iii) six SF systems. The ternary binders included four FAC-SF systems and five GGBS-SF systems. Three quaternary binders were prepared with FAC-SF-GGBS.

Figure 3 compares the MWC and RWD results of the 27 binder combinations, which are listed in Table 2. For the binary systems, the FAC and GGBS systems exhibited lower MWC values than that of the reference made with 100 % cement. The MWC value decreased with the increase of FAC's content due to the lubrication effects of FAC [31]. However, GGBS had an optimum amount that allowed the lowest MWC, due to its higher Blaine fineness than that of the cement, which improves the grain size distribution of the powder component and reduces the water demand [32]. However, GGBS has irregular shapes and large specific areas that may result in increase of the MWC. The MWC values of the SF binary systems were close to that of the reference mixture. The small and spherical SF particles can fill the voids between cement particles, which reduce the water demand. However, the fine SF particles are highly chemically reactive and can adsorb HRWR, which is adverse for the MWC [33].

Figure 3 indicates that the use of SCMs could increase the RWD and lead to a greater robustness. For the binary systems, the FAC60 mixture provided the smallest MWC, and the largest RWD. For the GGBS binary system, the G50 mixture had the best performance (smallest MWC and largest RWD). For the SF binary system, the SF5 mixture gave the best performance. For the GGBS-SF ternary systems, the use of 5 % SF slightly reduced the MWC and increased the RWD, compared with the corresponding GGBS binary systems. The fine SF particles filled the voids between the bigger cement and GGBS particles and formed gel that reduced the friction between the particles [32],

**Table 2** Codification of initial investigated binders (vol.%)

Group	Code	Cement	GGBS	FAC	SF
1	Ref	100	–	–	–
2	G40	60	40	–	–
	G50	50	50	–	–
	G60	40	60	–	–
	G70	30	70	–	–
3	FAC30	70	–	30	–
	FAC40	60	–	40	–
	FAC50	50	–	50	–
	FAC60	30	–	60	–
4	SF5	95	–	–	5
	SF8	92	–	–	8
	SF11	89	–	–	11
	SF14	86	–	–	14
	SF20	80	–	–	20
	SF25	75	–	–	25
5	FAC40SF5	55	–	40	5
	FAC50SF5	45	–	50	5
	FAC50SF8	42	–	50	8
	FAC60SF5	35	–	60	5
6	G40SF5	55	40	–	5
	G50SF5	45	50	–	5
	G60SF5	35	60	–	5
	G50SF8	42	50	–	8
	G50SF11	39	50	–	11
7	F40S5G10	45	10	40	5
	F40S5G20	35	20	40	5
	F40S5G30	25	30	40	5

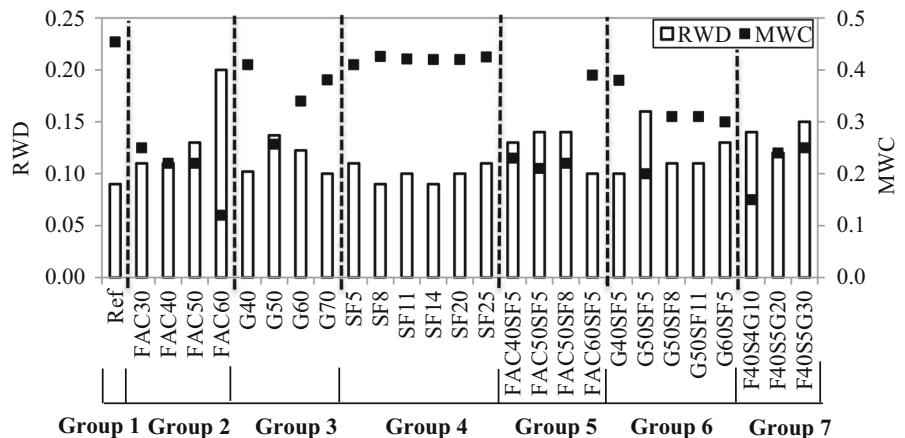
thus reducing the MWC. However, using 5 or 8 % SF in the FAC-SF ternary systems did not demonstrate significant improvement for the corresponding FAC binary systems. Particularly, the use of 5 % SF led to a notable increase in MWC and reduction in RWD when 60 % FAC was used. In summary, the G50SF5 mixture provided the highest packing density (smallest MWC) and robustness (largest RWD). All three quaternary systems offered relatively low MWC and high RWD, as indicated in Fig. 3.

Out of the 27 binder combinations shown in Fig. 3, 18 binders that have relatively low MWC (high packing density) were selected. Aside from Group 1 (shown in Table 1; Fig. 3), two combinations having the lowest MWC were selected in each group. For Groups 2, 4, 5, 6, and 7, three mixtures were selected since the second and third mixtures have similar performance.

4.1.2 Narrow down binder combinations based on key fresh and hardened properties for paste

In this step, the w/cm was fixed at 0.20. Figure 4 shows the results of HRWR demand (active solid material in HRWR divided by binder, wt.%), and 1- and 28-days compressive strengths of paste mixtures. Under standard curing, the FAC binary systems, except for the FAC60 mixture, achieved higher 1-days compressive strengths but lower 28-days compressive strengths than those of the GGBS binary systems. Using high-volume GGBS or FAC could lead to 75 % lower HRWR demand compared with the reference

**Fig. 3** Effect of binder type on minimum water content and relative water demand





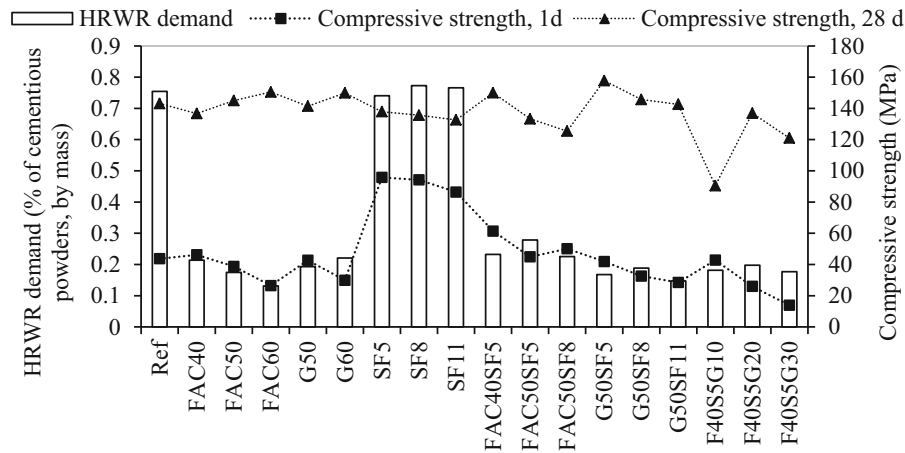


**Fig. 4** HRWR demand and 1- and 28-days compressive strength of paste

mixture. The use of SF did not influence the HRWR demand and 28-days compressive strength significantly but increased considerably the 1-days compressive strength. For example, the use of 5 % SF resulted in 95.8 MPa of the 1-days compressive strength which is more than twice that of the reference mixture (45.8 MPa). The SF binary systems demonstrated the highest 1-days compressive strength compared to other binary systems but also the highest HRWR demand. Except for the FAC40SF5G10 mixture, the 28-days compressive strength of the 17 binder combinations was in the range of 125–158 MPa. The HRWR demand of the binders with high-volume SCMs combinations was about one-third of those of the reference and the SF binary systems.

In this study, the weighted factors that were used in radar chart analysis were selected to secure high performance of UHPC intended for precast application. The factors for the 1-days compressive strength, 28-days compressive strength, MWC, flow time, RWD, and HRWR demand were 2, 4, 3, 3, 2 and 3, respectively. Figure 5 shows the area obtained from the radar charts. The FAC60 had the largest area, followed by G50SF5, G50, FAC40SF5, FAC40, and G50SF11 mixtures. The top six binder combinations were selected for evaluating the rheological properties.

#### 4.1.3 Finalize binders based on rheological properties for paste

Seven binder combinations, including the reference (Ref) and six candidates selected from the previous

steps, were further evaluated in terms of the rheological properties. Since the  $w/b$  and initial mini-slump flow were fixed for all mixtures, spreads of  $\mu_p$  at 20 min between the mixtures were mainly due to their differences in packing densities and water film thicknesses that depend on the HRWR dosage and binder in use Ferraris et al. [34]. Figure 6 shows the variation in  $\mu_p$  from 20 to 60 min after water addition. At 20 min, the G50SF5 mixture achieved the lowest  $\mu_p$ , whereas the reference paste had the highest  $\mu_p$ . A lower  $\mu_p$  of binders indicated more additional water amount, thicker water film, and lower friction between particles [35]. Between 20 and 60 min, the  $\mu_p$  values did not change significantly and had similar rates of increase in  $\mu_p$ .

Low  $\mu_p$  is desirable to achieve good filling capacity [36]. Relatively low  $\mu_p$  can also help fibers get evenly distributed in the matrix and improve the flexural performance. Mixtures that are highly viscous can entrap air, and, thus have reduced strength. Therefore, based on the results presented in Fig. 6, the G50SF5, FAC40SF5, G50, and FAC60 mixtures were selected for further evaluation.

#### 4.2 Preliminarily select a $w/cm$ for paste

A  $w/cm$  in the range of 0.18–0.23 was investigated for the four optimum binders. As indicated in Fig. 7, when the  $w/cm$  was increased from 0.18 to 0.23, the 28-days compressive strengths under standard curing did not decrease significantly (<10 %), but the HRWR demand was reduced by about 40–60 %. When the

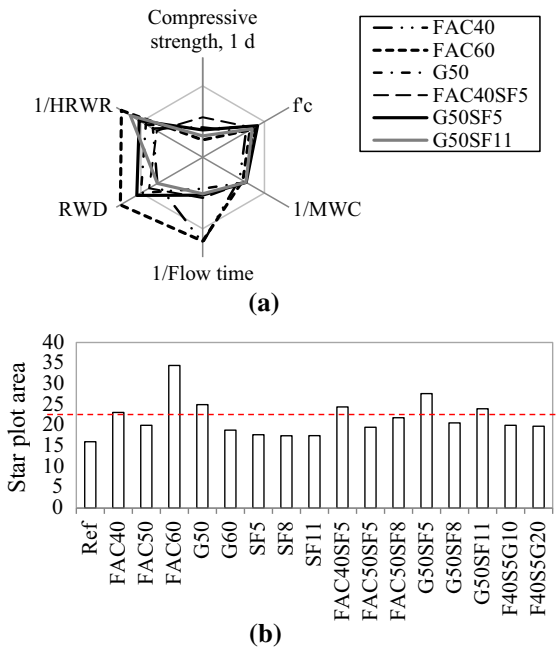


**Fig. 5** Multi-variable analysis: **a** radar chart and **b** areas in radar chart

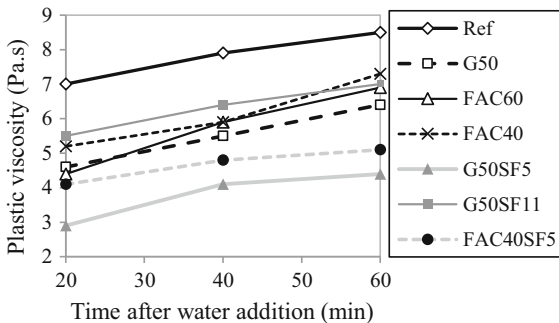


**Fig. 6** Time versus plastic viscosity of paste mixtures

w/cm was increased from 0.20 to 0.23, the HRWR demand did not change significantly. Therefore, a w/cm of 0.2 was preliminarily selected, which allowed high compressive strength and flowability and relatively small temperature change.

### 4.3 Determine sand combination

The  $D_{max}$  and  $D_{min}$  values were determined by the sieve sizes of 4.75 and 0.15 mm, respectively. The optimized sand combination can result in an optimized gradation curve that could be achieved with the minimum deviation from the target gradation curve,

as shown in Fig. 8. For the river sand and masonry sand employed in this study, the optimized sand combination to meet the targeted particle size distribution consisted of 70 % of river sand and 30 % of masonry, by mass.

In order to validate the suitability of the optimized sand to achieve high packing density, the densities of different sand combinations were measured using a gyrator compaction testing procedure. The combination with 70 % river sand and 30 % masonry indeed resulted in the highest bulk packing density ( $1870 \text{ kg/m}^3$ ) compared to the density of other sand blends.

By applying the Eqs. 3 and 4, the void content ( $\alpha$ ) can be determined as:  $\alpha = (1 - 1870/2640) \times 100 = 30$ . This value is required for evaluating the binder-to-sand volume ratio ( $V_b/V_s$ ).

### 4.4 Determine $V_b/V_s$

The minimum  $V_b/V_s$  is determined to be 0.6 according to Eqs. 5–8, where  $R_{S,A}$  equals 2 [29]. The flow properties and compressive strength for mortars with  $V_b/V_s$  values of 0.6, 0.7, 0.8, 0.9, 1.0 and 1.3 were tested, as shown in Table 3. The mixtures were prepared with the same binder made with 50 % GGBS, 5 % SF, and 45 % cement. The w/cm was set to 0.2. As  $V_b/V_s$  value was increased from 0.6 to 1.3, the HRWR demand and flow time were increased from 0.12 to 0.30 % and from 46 to 129 s, respectively. The corresponding 1-days compressive strength was increased from 40 to 42 MPa, respectively, and the 7- and 28-days compressive strengths were increased from 75 to 90 MPa and from 100 to 124 MPa, respectively. Therefore, as  $V_b/V_s$  value increased from 1.0 to 1.3, the compressive strength results did not change considerably, but the HRWR demand and flow time were significantly increased. The  $V_b/V_s$  value was determined to be 1.0, which resulted in optimized mixture with relatively low HRWR demand and viscosity, low paste content, and high compressive strength.

### 4.5 Determine fiber content

Short steel fibers were used to enhance the post-cracking performance. As the fiber content was increased from 0 to 2.5 % with a step size of 0.5 %, as shown in Table 4, the HRWR demand, which was



**Fig. 7** HRWR demand and compressive strength at 28 day for different w/cm values

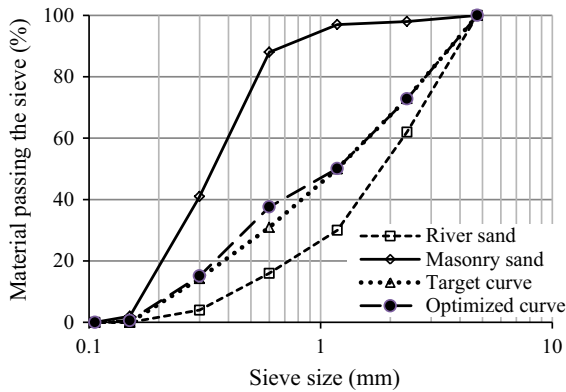
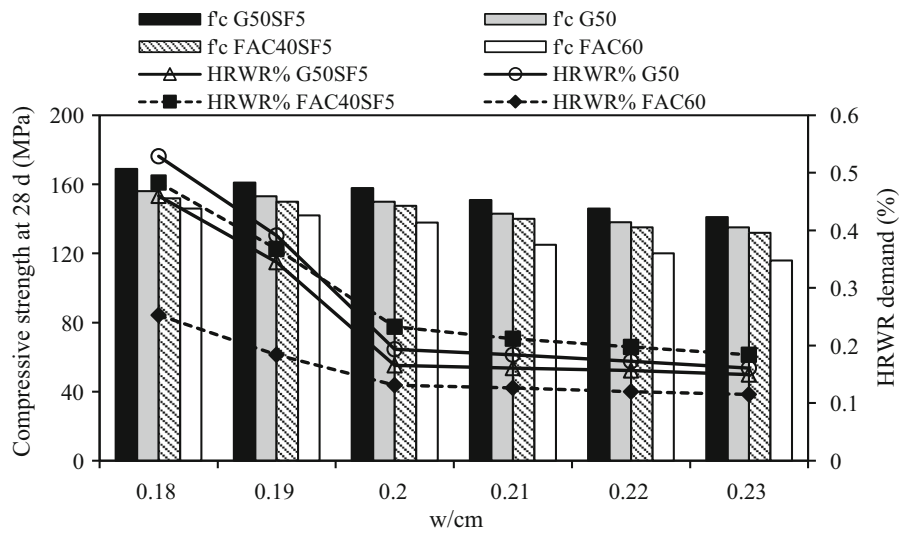


**Fig. 8** Sand gradations

required to ensure the slump flow of  $280 \pm 10$  mm was increased from 0.28 to 0.69 %, and the flow time was increased from 12 to 35 s. Particularly, when the fiber volume percentage, denoted by  $V_f$ , was increased

from 2 to 2.5 %, the HRWR dosage and flow time were increased by 72 and 94 %, respectively.

For the flexural properties, the first cracking load is expressed as  $f_1$ , which corresponds to the load at the appearance of the first crack, as shown in Table 3. The peak load is denoted by  $f_p$ . The mid-span deflections corresponding to  $f_1$  and  $f_p$  are denoted by  $\delta_1$  and  $\delta_p$ , respectively. The area under load versus deflection curve between deflection values of 0 to  $L/150$  ( $L = 202$  mm) is referred to as T150, which represents the toughness and is an indicator of energy dissipation. As the fiber content increased from 0 to 2 %, the  $f_1$  and  $f_p$  increased by 20 and 48 %, respectively. However, as the fiber content was further increased from 2 to 2.5 %, without significantly change in  $f_p$  and T150. A drop in  $f_1$  was observed. The highest  $f_p$  and T150 were secured by the use of 2 % steel fibers which is considered as the optimum fiber content.

**Table 3** Compressive strengths of different binder-to-sand ratio ( $V_b/V_s$ )

$V_b/V_s$	HRWR demand (%)	Flow time (s)	Compressive strength (MPa)		
			1 day	7 days	28 days
0.6	0.12	46	40	75	100
0.7	0.18	64	41	80	106
0.8	0.21	79	43	83	111
0.9	0.25	92	42	85	115
1.0	0.28	104	42	88	123
1.3	0.30	129	42	90	124

**Table 4** Performance of UHPC made with different fiber contents

Code	$V_f$ (%)	HRWR demand (%)	Slump flow (mm)	Flow time (s)	28-days compressive strength (MPa)	$f_1$ (MPa)	$\delta_1$ (mm)	$f_p$ (MPa)	$\delta_p$ (mm)	T150 (J)
Ref.-no fiber	0.0	0.28	29.0	12	123	13.7	0.10	13.7	0.10	1.0
Steel-0.5 %	0.5	0.28	29.0	20	124	14.9	0.10	14.9	0.10	24.5
Steel-1.0 %	1.0	0.28	28.5	22	124	15.9	0.07	16.5	0.61	38.4
Steel-1.5 %	1.5	0.29	28.0	24	125	16.2	0.11	19.6	0.77	41.3
Steel-2.0 %	2.0	0.40	28.0	18	125	16.5	0.08	20.3	1.05	50.2
Steel-2.5 %	2.5	0.69	28.0	35	126	12.7	0.07	19.7	1.65	49.7

#### 4.6 Evaluate and adjust the designed UHPC mixtures

Based on the above investigations, four mixtures were selected for further evaluation. Table 5 lists the four mixtures and a proprietary UHPC mixture taken as the reference mixture. These mixtures were prepared using the EIRICH mixer. The UHPC mixtures were designed to have a mini-slump flow diameter of  $280 \pm 10$  mm, by adjusting the HRWR dosage, without consolidation. The w/cm was not changed since all the mixtures achieved 28-days compressive strengths higher than 120 MPa under standard curing.

##### 4.6.1 Fresh and physical properties

Table 6 summarizes the results of fresh properties. All the mixtures were self-consolidating and stable. The mini V-funnel flow times and plastic viscosities of the mixtures ranged from 12 s to 46 s and 23–50 Pa, respectively. The reference mixture exhibited the lowest flow time and plastic viscosity, which were 12 s and 23 Pa.s, respectively. The highest flow time and plastic viscosity, which were 46 s and 50 Pa.s, respectively, were obtained by the G50 mixture. The HRWR demands of all the mixtures were in the range of 0.5–1.4 %. The HRWR demand was the lowest for the FAC60 mixture and the highest for the G50SF5

mixture. The FAC40SF5 mixture demonstrated the longest initial setting time of 10 h and final setting time of 15 h. The G50SF5 had the shortest initial and final setting time of 2 h and 6 h, respectively.

##### 4.6.2 Compressive strengths

Compressive strengths of the selected mixtures at 28 days under standard and heat curing methods were compared, as listed in Table 6. The 28-days compressive strength of the reference mixture was 135 MPa and that of the designed mixtures was up to 125 MPa, under standard curing. The designed mixtures had slightly lower compressive strengths than that of the reference mixture. This may be due to the low silica fume content of the designed UHPC mixtures compared with the reference mixture. The designed UHPC mixtures achieved 28-days compressive strength up to 178 MPa under heat curing, which was 12 % lower than that of the reference UHPC (202 MPa). The FAC60 mixture had 136 MPa under initial heat curing, which is under the target value of 150 MPa.

##### 4.6.3 Unit cost per compressive strength under standard curing

The unit cost per strength, defined as the ratio of the unit cost ( $\$/m^3$ ) normalized by the 28-days

**Table 5** Proportioning of the designed UHPC mixtures (unit:  $kg/m^3$ )

Code	Cemen	SF	FAC	GGBS	Quartz sand	Fine sand	Sand A	Sand B	HRWR	Total water	Steel fibers
Ref.	712	231	–	–	1020	211	–	–	6.5	164	156
G50SF5	548	42	–	535	–	–	694	304	16.0	167	156
G50	593	–	–	546	–	–	698	295	12.5	182	156
FAC40SF5	663	42	367	–	–	–	703	308	12.0	171	156
FAC60	486	–	556	–	–	–	715	304	5.5	188	156



**Table 6** Characteristics of the UHPC mixtures

Code	Ref.	G50SF5	G50	FAC40SF5	FAC60
Flow time (s)	12	30	37	39	46
HRWR demand (%)	0.69	1.38	1.06	1.01	0.51
Mini slump flow (mm)	275	280	285	285	285
Yield stress (Pa)	39	35	37	34	30
Plastic viscosity (Pa s)	23	39	50	44	29
Air content (%)	4	5	5	4	3.5
Specific gravity	2.47	2.45	2.43	2.44	2.41
Initial setting (h)	5	2	6	10	6
Final setting (h)	10	6	12	15	12
1 days—standard curing (MPa)	53	52	64	65	69
28 days—standard curing (MPa)	135	125	124	124	120
28 days—heat curing (MPa)	202	178	170	168	136
Splitting tensile strength (MPa)	12	14	12	12	10
Unit costs normalize by compressive strength (\$/m <sup>3</sup> /MPa)	14.8	4.7	4.2	4.3	3.5
Modus of elasticity (GPa)	53	50	50	52	46
Flexural performance					
First cracking load (kN)	22	21	24	21	20
Peak load (kN)	21	29	33	31	28
$\delta_1$ (mm)	0.092	0.085	0.080	0.093	0.089
$\delta_p$ (mm)	0.701	0.690	0.653	0.820	0.635
Peak strength (MPa)	19.7	20.2	22.8	21.3	20.1
T150 (J)	40.4	48.8	51.5	51.1	49.4
Surface conductivity (k $\Omega$ cm)	45	30	28	38	34
Durability factor (%)	99.8	99.8	99.8	99.7	99.7
Autogenous shrinkage at 28 days ( $\mu$ m/m)	731	602	253	545	593
Drying shrinkage at 98 days ( $\mu$ m/m)	600	430	56	466	500

compressive strength under standard curing conditions, as shown in Table 6. The unit cost includes the costs of all ingredients necessary for producing the UHPC mixtures in exception of transportation cost. The unit cost of the selected cement, SF, FAC, GGBS, local river sand, masonry sand, quartz sand, HRWR, and steel fiber are 0.2, 0.66, 0.03 0.05, 0.014, 0.007, 2.2, 3.8 and 1.0 \$/kg, respectively. These costs apply to St. Louis, MO, in 2016. The FAC and GGBS have 75 % lower unit cost than the cement. The local river sand has about 99.5 % lower unit cost than the special finely-ground quartz sand. Thus, the use of high-volume SCMs and local river sand could significantly reduce the unit cost of the UHPC. The unit cost per strength was 14.8 \$/m<sup>3</sup>/MPa for the reference mixture, and 3.5, 4.2, 4.3 and 4.7 \$/m<sup>3</sup>/MPa for the designed FAC 60, G50, FAC40SF5, and G50SF5 mixtures,

respectively. This corresponds to 68–76 % reduction in unit cost per unit compressive strength.

#### 4.6.4 Other mechanical properties

Table 6 summarizes the test results of the splitting tensile strength, Young's modulus, and flexural properties of the investigated UHPC mixtures under standard curing. The G50SF5 and FAC60 mixtures offered the highest and the lowest splitting tensile strengths of 14.3 and 10.3 MPa, respectively. The FAC40SF5 and FAC60 gave the highest and the lowest elastic moduli of 51.6 and 45.8 GPa, respectively. For the flexural properties, the flexural strengths of the five mixtures were close and ranged from 19.7 to 22.8 MPa. The G50 mixture had the highest first cracking and peak loads and toughness.



The reference mixture had the lowest flexural strength and T150.

#### 4.6.5 Shrinkage

Autogenous shrinkage, which is caused by volume reduction due to chemical reactions during hydration and self-desiccation, contributes mostly to the total shrinkage in UHPC [37]. Table 6 shows the results of 28-days autogenous shrinkage measured since the final setting. The reference mixture had the highest 28-days autogenous shrinkage, which was 730  $\mu\text{m}/\text{m}$ , due to the high silica fume content. The lowest autogenous shrinkage of 250  $\mu\text{m}/\text{m}$  was obtained by the G50 mixture. The G50SF5, FAC60 and FAC40SF5 mixtures had 28-days autogenous shrinkage values of 600, 595 and 545  $\mu\text{m}/\text{m}$ , respectively.

The drying shrinkage values measured after 7 days of moist curing. The end of the moist curing was chosen as “time zero” ( $t = 0$ ). The reference mixture reached a total drying shrinkage of 600  $\mu\text{m}/\text{m}$ , which was the highest value compared with the other designed mixtures. The G50 mixture displayed the minimum drying shrinkage, which was only 55  $\mu\text{m}/\text{m}$ . The total shrinkage of the UHPC can be considered as the initial autogenous shrinkage after 7 days, when autogenous shrinkage was stabilized, plus the drying shrinkage determined following 7 days of moist curing. The G50 mixture had the lowest total shrinkage of 310  $\mu\text{m}/\text{m}$ . The reference mixture obtained the highest total shrinkage, which was 1330  $\mu\text{m}/\text{m}$ .

#### 4.6.6 Durability

**4.6.6.1 Electrical resistivity** The electrical resistivity affects the corrosion resistance of the material. Test results of surface resistivity, which is an indicator of electrical resistivity, of the five UHPC mixtures determined at 28 days, are shown in Table 6. Mixtures with a surface conductivity greater than 20  $\text{k}\Omega\text{ cm}$  can be considered to have a low risk of corrosion rate [38]. Hence, all the mixtures that had surface conductivities of 30–38  $\text{k}\Omega\text{ cm}$  can be considered to exhibited a low risk of corrosion rate. The reference mixture with high silica fume content had the highest electrical resistivity. The G50 mixtures had the lowest electrical resistivity.

**4.6.6.2 Freezing and thawing** The variations in durability factor of the UHPC mixtures after 300 freeze–thaw cycles are shown in Table 6. All the UHPC mixtures exhibited adequate resistance to freezing and thawing with durability factors of nearly 100 %. The freezing and thawing testing was initiated after 56 days of moist curing given the high volume of SCMs. The excellent frost durability is associated with the very low permeability of the material.

## 5 Conclusions

A mix design methodology is presented for producing cost-effective UHPC with high-volume SCMs and conventional concrete sand. Based on the reported studies, the following conclusions can be drawn:

- (1) The MWC can first be used as an indicator of the packing density of binders in wet condition to narrow down binder systems and reduce the required number of experiments. The binder composition of UHPC can then be optimized with consideration on the HRWR demand, rheological properties, MWC, RWD, and compressive strength properties. A radar chart can be then employed for the analysis. Based on this approach the following binder combinations were selected: G50, G50SF5, FAC60, and FAC40SF5.
- (2) The second step is to determine the preliminary  $w/\text{cm}$  based on the 28-days compressive strength and HRWR demand value for paste mixtures prepared with the optimum binder combinations with  $w/\text{cm}$  values of 0.18–0.23. The optimum value for the selected binders was 0.20.
- (3) The modified Andreasen and Andersen model can be used to optimize sand gradation. In this study, 70 % river sand and 30 % masonry sand were selected to achieve the highest packing density.
- (4) The next step involves the determination of the binder-to-sand volume ratio ( $V_b/V_s$ ). Mortar mixtures made with the selected  $w/\text{cm}$  and G50SF5 binder were prepared with  $V_b/V_s$  values of 0.6, 0.7, 0.8, 0.9, 1.0 and 1.3. Based on flow properties and 28-days compressive strength, the optimum  $V_b/V_s$  was determined to be 1.0.



- (5) The optimum fiber content for the UHPC is experimentally determined given the flowability and flexural properties of UHPC made with various fiber contents. For the steel fibers considered in this study, 2 % fiber volume was selected.
- (6) For the UHPC mixtures prepared with the various binder systems and optimized mixture proportioning, the UHPC mixtures were self-consolidating, stable, and had 28-days compressive strengths of 120–125 MPa under standard curing condition. The strength can reach up to 178 MPa by applying heat curing at a maximum temperature of 90 °C for one day followed by 7-days moist curing. For the selected UHPC mixtures, the 28-days splitting tensile strength, modulus of elasticity, flexural strength, and toughness (T150) were 11.6–14.3 MPa, 48.8–51.6 MPa, 20.2–21.3 MPa and  $50 \pm 1.5$  kN mm, respectively.
- (7) The designed UHPC mixtures exhibited relatively low autogenous shrinkage and drying shrinkage. The G50 mixture had the lowest autogenous and drying shrinkage of 255  $\mu\text{m}/\text{m}$  at 28 days and 55  $\mu\text{m}/\text{m}$  at 98 days, respectively. All tested UHPC mixtures exhibited a very high electrical resistivity and excellent frost durability.
- (8) The unit cost per compressive strength of the UHPC mixtures designed with high volume of SCMs and concrete sand can range between 4.1 and 4.7  $\$/\text{m}^3/\text{MPa}$ . The mixture FAC60 was the most cost-effective mixture, which also developed better workability and lower unit cost per compressive strength of 3.7  $(\$/\text{m}^3)/\text{MPa}$  than other mixtures.

**Acknowledgments** This study was funded by the Energy Consortium Research Center of Missouri S&T under Grant No. SMR-1406-09 and the RE-CAST University Transportation Center at Missouri University of S&T under Grant No. DTRT13-G-UTC45. Certain commercial equipment, instruments, or materials are identified in this paper only in order to specify the experimental procedure.

## References

1. De Larrard F, Sedran T (1994) Optimization of ultra-high-performance concrete by the use of a packing model. *Cem Concr Res* 24(6):997–1009
2. Richard P, Cheyrezy M (1995) Composition of reactive powder concretes. *Cem Concr Res* 25:1501–1511
3. Brihwiler E, Denarié E (2008) Rehabilitation of concrete structures using ultra-high performance fibre reinforced concrete. In: Proceedings of the second international symposium on ultra high performance concrete, Kassel, pp 1–8
4. Habert G, Denarié E, Šajna A, Rossi P (2013) Lowering the global warming impact of bridge rehabilitations by using ultra high performance fibre reinforced concretes. *Cem Concr Compos* 38:1–11
5. Yu R, Spiesz P, Brouwers HJH (2014) Mix design and properties assessment of Ultra-High Performance Fibre Reinforced Concrete (UHPFRC). *Cem Concr Res* 56:29–39
6. El-Dieb AS (2009) Mechanical, durability and microstructural characteristics of ultra-high-strength self-compacting concrete incorporating steel fibres. *Mater Des* 30:4286–4292
7. Hassan AMT, Jones S, Mahmud GH (2012) Experimental test methods to determine the uniaxial tensile and compressive behaviour of Ultra-High Performance Fibre Reinforced Concrete (UHPFRC). *Constr Build Mater* 37:874–882
8. Wang C, Yang C, Liu F, Wan C, Pu X (2012) Preparation of ultra-high performance concrete with common technology and materials. *Cem Concr Compos* 34:538–544
9. Wille K, Naaman AE, Parra-Montesinos GJ (2011) Ultra-high performance concrete with compressive strength exceeding 150 MPa (22 ksi): a simpler way. *ACI Mater J* 108:45–54
10. Wille K, Naaman AE, El-Tawil S (2011) Optimizing ultra-high-performance fiber-reinforced concrete. *Concr Int* 33:35–41
11. Yang SL, Millard SG, Soutsos MN, Barnett SJ, Le TT (2009) Influence of aggregate and curing regime on the mechanical properties of ultra-high performance fibre reinforced concrete (UHPFRC). *Constr Build Mater* 2:2291–2298
12. Le HT, Müller M, Siewert K, Ludwig HM (2015) The mix design for self-compacting high performance concrete containing various mineral admixtures. *Mater Des* 72:51–62
13. Graybeal B (2011) Ultra-high performance concrete. FHWA-HRT-11-038. FHWA, U.S. Department of Transportation
14. Khayat KH, Mitchell D, Long WJ, Lemieux G, Hwang SD, Yahia A, Cook WD, Baali L (2007) Self-consolidating concrete for precast, prestressed concrete bridge elements. NCHRP Project 18–12. University of Sherbrooke, Quebec
15. Richard P, Cheyrezy M (1994) Reactive powder concretes with high ductility and 200–800 MPa compressive strength. *ACI Mater J* 144:507–518
16. Dils J, Boel V, De Schutter G (2015) Vacuum mixing technology to improve the mechanical properties of ultra-high performance concrete. *Mater Struc* 48:3485–3501
17. Funk JE, Dinger DR (1994) Predictive process control of crowded particulate suspension. Applied to ceramic manufacturing. Kluwer Academic Press, New York
18. Yu R, Spiesz P, Brouwers HJH (2015) Development of an eco-friendly Ultra-High Performance Concrete (UHPC) with efficient cement and mineral admixtures uses. *Cem Concr Compos* 55:383–394



19. Li LG, Kwan AKH (2014) Packing density of concrete mix under dry and wet conditions. *Powder Tech* 253:514–521
20. Iveson SM, Litster JD, Hapgood K, Ennis BJ (2001) Nucleation, growth and breakage phenomena in agitated wet granulation processes: a review. *Powder Tech* 117:3–39
21. Tomas J (2004) Fundamentals of cohesive powder consolidation and flow. *Granular Matter* 6:75–86
22. Wu Q, An XH (2014) Development of a mix design method for SCC based on the rheological characteristics of paste. *Constr Build Mater* 53:642–651
23. Hwang SD, Khayat KH (2006) Effect of various admixture-binder combinations on workability of ready-mix self-consolidating concrete. *ACI Mater J* 233:25–44
24. Dudziak L, Mechtcherine V (2008) Mitigation of volume changes of ultra-high performance concrete (UHPC) by using super absorbent polymers. In: *Proceedings of the second international symposium on ultra high performance concrete*, Kassel, pp 425–432
25. EFNARC (2002) Specification and guidelines for self-compacting concrete, English edn. European Federation for Specialist Construction Chemicals and Concrete Systems, Norfolk
26. Khayat HK, Kassimi F, Ghoddousi P (2014) Mixture design and testing of fiber-reinforced self-consolidating concrete. *ACI Mater J* 111:143–152
27. Tattersall GH, Banfill PFG (1983) *Rheology of fresh concrete*. Pitman, London
28. Li LG, Kwan AKH (2011) Mortar design based on water film thickness. *Constr Build Mater* 25:2381–2390
29. Koehler E, Fowler D (2007) Aggregate in self-consolidating concrete. In: ICAR project 108. The University of Texas at Austin: International Center for Aggregates Research
30. Park SH, Kim DJ, Ryu GS, Koh KT (2012) Tensile behavior of ultra-high performance hybrid fiber reinforced concrete. *Cem Concr Compos* 34:172–184
31. Termkhajornkit P, Nawa T, Ohnuma H (2001) Effects of properties of fly ash on fluidity of paste. *Cem Sci Concr Technol* 55:163–169
32. Parka CK, Nohb MH, Parkb TH (2005) Rheological properties of cementitious materials containing mineral admixtures. *Cem Concr Res* 35:842–849
33. Otsubo Y, Miyai S, Umeya K (1980) Time-dependent flow of cement paste. *Cem Concr Res* 10:631–638
34. Ferraris CF, Obla KH, Hill R (2001) The influence of mineral admixtures on the rheology of cement paste and concrete. *Cem Concr Res* 31:245–255
35. Wong HHC, Kwan AKH (2008) Rheology of cement paste: role of excess water to solid surface area ratio. *J Mater Civil Eng, ASCE* 20:189–197
36. Mechtcherine V, Secrieru E, Schröf C (2015) Effect of superabsorbent polymers (SAPs) on rheological properties of fresh cement-based mortars Development of yield stress and plastic viscosity over time. *Cem Concr* 67:52–65
37. Bao Y, Meng W, Chen Y, Chen G, Khayat KH (2015) Measuring mortar shrinkage and cracking by pulse pre-pump Brillouin optical time domain analysis with a single optical fiber. *Mater Lett* 145:344–346
38. Broomfield J (2011) Measuring concrete resistivity to assess corrosion rates. *Concrete Report from the Concrete Society/Institute of Corrosion Liaison Committee*, pp 37–39

